

ATDC (Ataxia Telangiectasia Group D Complementing) Promotes Radioresistance through an Interaction with the RNF8 Ubiquitin Ligase*

Received for publication, May 26, 2015, and in revised form, September 9, 2015. Published, JBC Papers in Press, September 17, 2015, DOI 10.1074/jbc.M115.665489

Huibin Yang^{‡§1}, Phillip L. Palmbo^{§¶1}, Lidong Wang^{‡§}, Evelyn H. Kim[‡], Gina M. Ney^{§||}, Chao Liu[¶], Jayendra Prasad^{§**}, David E. Misek[‡], Xiaochun Yu[¶], Mats Ljungman^{§**}, and Diane M. Simeone^{‡§¶#2}

From the Departments of [‡]Surgery, [¶]Internal Medicine, ^{||}Pediatrics, ^{**}Radiation Oncology, ^{**}Molecular and Integrative Physiology, and [§]Translational Oncology Program, University of Michigan, Ann Arbor, Michigan 48109

Background: ATDC/TRIM29 promotes resistance to ionizing radiation, but the factor(s) that mediate this effect are incompletely understood.

Results: ATDC/TRIM29 binds to RNF8, promoting DNA repair and resistance to IR.

Conclusion: Following DNA damage, ATDC/TRIM29 is phosphorylated and interacts with RNF8, promoting DNA repair and cell survival.

Significance: The interaction between ATDC/TRIM29 and RNF8 is novel and is important for the DNA damage response.

Induction of DNA damage by ionizing radiation (IR) and/or cytotoxic chemotherapy is an essential component of cancer therapy. The ataxia telangiectasia group D complementing gene (*ATDC*, also called *TRIM29*) is highly expressed in many malignancies. It participates in the DNA damage response downstream of ataxia telangiectasia-mutated (ATM) and p38/MK2 and promotes cell survival after IR. To elucidate the downstream mechanisms of ATDC-induced IR protection, we performed a mass spectrometry screen to identify ATDC binding partners. We identified a direct physical interaction between ATDC and the E3 ubiquitin ligase and DNA damage response protein, RNF8, which is required for ATDC-induced radioresistance. This interaction was refined to the C-terminal portion (amino acids 348–588) of ATDC and the RING domain of RNF8 and was disrupted by mutation of ATDC Ser-550 to alanine. Mutations disrupting this interaction abrogated ATDC-induced radioresistance. The interaction between RNF8 and ATDC, which was increased by IR, also promoted downstream DNA damage responses such as IR-induced γ -H2AX ubiquitination, 53BP1 phosphorylation, and subsequent resolution of the DNA damage foci. These studies define a novel function for ATDC in the RNF8-mediated DNA damage response and implicate RNF8 binding as a key determinant of the radioprotective function of ATDC.

Anticancer treatments such as ionizing radiation (IR)³ induce DNA damage (including both single-strand and double-strand breaks (DSB)), which activates a complex DNA damage response (DDR) program. This DDR coordinates cell cycle checkpoint activation, transcriptional regulation, and DNA repair, resulting in either restoration of the genome and cell survival or induction of programmed cell death in a process known as apoptosis (1). A key component of the DDR is the phosphorylation of H2AX primarily by ATM, ATR (ataxia telangiectasia and Rad3-related), and DNA-PK at sites of DNA DSB, resulting in subsequent recruitment of DNA repair and chromatin-modifying enzymes. This recruitment process requires a series of chromatin and repair enzyme covalent modifications including ubiquitination and sumoylation (2).

RNF8 is a crucial component of the DDR. RNF8, an E3 ubiquitin ligase, catalyzes the addition of poly-ubiquitin chains to H2AX and the DNA DSB repair complex, Mre11-Rad50-NBS1 (1). RNF8 is recruited to DNA damage sites by the binding of its forkhead-associated (FHA) domain to ATM-phosphorylated MDC1 (3, 4). Once recruited, RNF8 catalyzes poly-ubiquitination of downstream repair proteins such as RAP80, 53BP1, and BRCA1, which allows their recruitment to the DNA DSB to facilitate DNA repair (5).

Ataxia telangiectasia group D complementing (*ATDC*), also known as *TRIM29*, was identified for its capacity to induce resistance to IR in cells derived from patients with ataxia telangiectasia, a disorder characterized by ATM deficiency (6). *ATDC* (*TRIM29*) is a member of the tripartite motif (TRIM) protein family, which is defined by a conserved RING domain, one or two B-box domains, and a coiled-coil region (7). *ATDC* does not have a RING domain, but does have typical B-box and

* This work was funded by grants from the Pardee Foundation (to D. M. S.), National Institutes of Health Grants R01 CA13104505A1 and CA17483601A1 (to D. M. S.), National Institutes of Health Grant T32 CA009357 (to P. L. P.), American Society of Clinical Oncology (ASCO) Young Investigator Award (to P. L. P.), and the Bladder Cancer Advocacy Network (BCAN) Miriam Gleberman Young Investigator Award (to P. L. P.). The authors declare that they have no conflicts of interest with the contents of this article.

¹ Both authors contributed equally to this work.

² To whom correspondence should be addressed: Depts. of Surgery and Molecular and Integrative Physiology, Translational Oncology Program, TC 2922D, Box 0331, University of Michigan Medical School, 1500 E. Medical Center Dr., Ann Arbor, MI 48109. Tel.: 734-615-1600; Fax: 734-936-5830; E-mail: simeone@med.umich.edu.

³ The abbreviations used are: IR, ionizing radiation; ATDC, ataxia telangiectasia group D complementing; ATM, ataxia telangiectasia-mutated; DDR, DNA damage response; DSB, double-strand breaks; TRIM, tripartite motif; FHA, forkhead-associated; H2AX, H2A histone family, member X; co-IP, co-immunoprecipitation; TPCK, L-1-tosylamido-2-phenylethyl chloromethyl ketone; CC, coiled-coil; PARP, poly(ADP-ribose) polymerase; Gy, grays.

coiled-coil domains. ATDC is known to physically interact with the intermediate filament protein, vimentin, as well as the proteins hPKC1-1, p53, HDAC9, and Tip60 (8–12).

Interestingly, ATDC is highly expressed in multiple tumor types and is typically a marker of invasive/aggressive tumors (13–16). In pancreatic cancer cells, ATDC has been shown to interact with DVL-2 through its coiled-coil domain, leading to the promotion of cell proliferation and invasion (17). ATDC also binds to p53, influencing cell cycle progression (10, 17). We have recently demonstrated that ATDC is a downstream phosphorylation target of ATM and MAPKAPK2 (MAPK-activated protein kinase 2) following exposure to IR. Phosphorylation of ATDC is required to mediate resistance to IR (17). ATDC has also been shown to bind to chromatin and activate the DDR following DSB formation (18). The mechanism(s) downstream of ATDC that mediate radioresistance, however, are not known.

In this study, we performed a mass spectrometry screen to identify ATDC binding partners and elucidated the downstream mechanisms by which ATDC mediated radioresistance. We describe a direct protein-protein interaction between ATDC and RNF8 that is enhanced by DNA damage. The interaction between ATDC and RNF8 promoted ATDC trafficking to the nucleus and enhanced DNA DSB repair, γ H2AX monoubiquitination, 53BP1 phosphorylation, and foci recovery of RNF8 and BRCA1 after IR treatment. Our results demonstrate a novel interaction between ATDC and RNF8 and reveal novel mechanistic insight into how this interaction participates in the radioprotective role of ATDC.

Experimental Procedures

Cells and Antibodies—HEK 293 cells were maintained in DMEM supplemented with 10% FBS and penicillin and streptomycin. The HEK 293 and human pancreatic ductal adenocarcinoma cell lines Panc1, BxPc3, and CAPAN2 were purchased from ATCC (Manassas, VA). The bladder cancer cell line, UC14, was obtained from Monica Liebert and subjected to DNA fingerprinting to confirm identity (19). All cells were grown in DMEM or RPMI 1640. Monoclonal anti-FLAG-tagged antibody was purchased from Sigma. H2AX-, γ H2AX-, and Myc-tagged antibodies were purchased from Cell Signaling (Danvers, MA). An anti-BRCA1 antibody was purchased from Millipore (Billerica, Massachusetts). Polyclonal anti-53BP1 and anti-p53BP1 antibodies were purchased from Bethyl Laboratories, Inc. (Montgomery, TX). Monoclonal anti-ATDC (B2), anti-H3, and anti-BRCA1 antibodies were obtained from Santa Cruz Biotechnology (San Jose, CA). The polyclonal anti-RNF8 antibody used was described previously (20). HEK 293 cell lines with stable expression of ATDC and its C-terminal deletion mutant have been described previously (17).

Constructs—The cDNA of human ATDC was kindly provided by J. Murnane (University of California, San Francisco). The full-length cDNA and the N-terminal or C-terminal truncation mutants of ATDC were subcloned into N-terminal p3 \times FLAG-CMV expression vector as described previously (17).

Cell Fractionation—Nuclear, cytoplasmic, membrane, and cytoskeleton proteins were extracted using a compartmental

protein extraction kit (Millipore, Billerica, Massachusetts) according to manufacturer's instructions.

Chromatin Extraction—HEK 293 cells expressing either ATDC or ATDC Δ C (lacking amino acids 348–588) were irradiated with 10 Gy and incubated for different times (1, 3, 6, and 24 h). Proteins bound to chromatin were released by treatment with 0.2 N HCl and analyzed by Western blotting.

Western Blot Analysis—Cells expressing full-length or deletion mutants of ATDC or RNF8 were lysed in cell lysis buffer (50 mM Tris-HCl, pH 8.0, containing 1% Triton X-100, 25 μ g/ml aprotinin and leupeptin, 1 mM PMSF, and 10% glycerol). The cell lysates were then centrifuged at 10,000 \times g for 10 min to remove debris. Protein concentrations were measured using the Bradford assay (Bio-Rad). Proteins separated by SDS-PAGE were transferred to nitrocellulose membranes. After blocking with blocking buffer (Tris-buffered saline (TBS), pH 7.4, with 0.1% Tween 20 (TBST) containing 5% skim milk powder) for 1 h at room temperature, the membranes were incubated for 1 h at room temperature with primary antibody. After incubation with secondary antibodies conjugated with HRP, the proteins were visualized using an ECL detection kit (Thermo Scientific).

Co-immunoprecipitation—Cells were transiently transfected with plasmids for expression of FLAG-tagged ATDC, Myc-tagged RNF8, or their various deletion mutants. Cells were resuspended in ice-cold lysis buffer (50 mM Tris, 150 mM NaCl, 0.5% IGEPAL, pH 7.4) containing freshly added protease inhibitors (Roche Applied Science, Mannheim, Germany) and sonicated for 5 s. The lysates were centrifuged for 15 min at 10,000 \times g to remove debris. As described previously, FLAG-tagged ATDC or Myc-tagged RNF8 was immunoprecipitated by incubating with anti-FLAG, anti-ATDC (B2, Santa Cruz Biotechnology), or anti-Myc antibodies and protein G-agarose beads (Gibco, Life Technologies) at 4 $^{\circ}$ C overnight (17). Immunoprecipitates were washed four times with ice-cold lysis buffer and resolved by reducing SDS-PAGE. Co-immunoprecipitated ATDC and its mutants were detected with anti-FLAG antibody (Sigma) or anti-ATDC antibody (Santa Cruz Biotechnology). Co-immunoprecipitated RNF8 or its mutants were detected with anti-Myc antibody (Cell Signaling).

Trypsin Digestion—HEK 293 cells were transfected with FLAG-ATDC expression vector or control vector. 24 h after transfection, cell lysates were made and subjected to immunoprecipitation with anti-FLAG conjugated to agarose beads. The bound proteins were eluted with 50 mM ethanolamine at pH 11.5 or 50 mM glycine buffer at pH 2.5. The eluates were lyophilized to 20- μ l volume. Proteins were reduced with 10% (v/v) DTT at 60 $^{\circ}$ C for 30 min and then alkylated with 15 mM iodoacetamide in the dark at room temperature for 30 min. A 1:20 ratio of TPCK-treated trypsin (Promega, Madison, WI) was added to each sample, and the samples were vortexed and then incubated at 37 $^{\circ}$ C overnight. The tryptic digestion was terminated by the addition of 2.5% v/v TFA.

LC-MS Analysis—Peptides from a tryptic digest of each sample were analyzed using a nano-LC/MS system consisting of an HPLC NanoACQUITY system (Waters). A C12 trap column (Jupiter Proteo-Phenomenex; particle size 90 \AA , 75 μ m \times 3 cm) was utilized before analytical column for desalting at a flow rate 10 μ l/min. 30- μ l aliquots of the peptide solutions were loaded

ATDC Interaction with RNF8

for each run. The trapped peptides were separated on an analytical column (Jupiter Proteo-Phenomenex: particle size 90 Å, 75 μm \times 25 cm, C12) with a 300 nl/min flow rate \times 1-h acetonitrile gradient. The mobile phases A and B were 0 and 100% acetonitrile, respectively, each containing 0.1% formic acid. The gradient began at 5% B and was ramped to 18% B by 32 min, to 35% by 47 min, to 50% by 50 min, and finally to 80% by 52 min. In each mass analysis, one high mass resolution (60,000 full width at half maximum) MS spectra was acquired and scanned from 300–1600 m/z in MS mode, followed by analysis of the 15 most abundant data-dependent MS/MS analyses (with dynamic exclusion for 45 s) throughout the collision-induced dissociation phase.

Collected MS/MS spectral data were analyzed for identification using the following analysis protocols. MS/MS spectra were searched with Mascot (version 2.3.02) under the conditions of 10 ppm parent ions mass tolerances, 0.8 Da product ion mass tolerances, and two missed cleavages. Carbamidomethylated cysteine (fixed), and Oxidation (M), N-acetyl (N-term), Deamidation (N,Q), Pyro-Glu (Q) (variable) were chosen as modifications.

Immunofluorescent Staining—HEK 293 cells expressing FLAG-tagged ATDC or ADTC Δ C were treated with ionizing radiation with 4 Gy and analyzed using immunofluorescence assays at the indicated time points after IR using antibodies against 53BP1 and BRCA1 at a dilution of 1:200 or RNF8 at a 1:500 dilution.

Pulldown Assays—*Escherichia coli* transformed with an inducible expression vector for RNF8 were cultured at 37 °C, until A_{600} reached \sim 0.8, and then 1 mM isopropyl- β -D-1-thiogalactopyranoside was added for an overnight incubation at room temperature to induce RNF8 expression. The bacteria were harvested and lysed by sonication on ice in 50 mM Tris-Cl (pH 8.0), 150 mM NaCl, 0.2% sodium deoxycholate, and 0.1% Triton X-100. The lysate was cleared by centrifugation, and RNF8 prebound glutathione-Sepharose beads were prepared according to protocol as described previously (21). FLAG-ATDC was *in vitro* translated directly from the PCR products that contain the T7 promoter by TNT quick coupled transcription/translation system according to manufacturer's protocol (Promega). Pulldown reactions were then initiated by the addition of GST-RNF8 or GST prebound to glutathione-Sepharose beads to *in vitro* translated products or lysates of HEK 293 cells with stable expression of ATDC. After rocking overnight at 4 °C, the beads were washed three times with TBS containing 250 mM NaCl and 0.25% Triton X-100 and analyzed by Western blotting.

Comet Assays—ATDC- or ATDC Δ C-expressing HEK 293 cells growing in complete DMEM medium at 80% confluence were irradiated (15 Gy). DNA double-strand repair was analyzed in neutral comet assays using the Trevigen comet assay kit (4250-050-K) according to the manufacturer's instructions.

Statistical Analysis—Data are represented as mean \pm S.E. or S.D. as indicated from at least three independent experiments. Significance of differences between groups was evaluated by Student's *t* test or analysis of variance. $p < 0.05$ was considered statistically significant.

Results

ATDC Binds Directly to RNF8—To better characterize the biological function of ATDC, we performed a screen to identify ATDC binding partners by affinity purification and mass spectrometric analysis. FLAG-tagged ATDC was expressed in HEK 293 cells (which have no endogenous ATDC expression), and trypsin-digested immunoprecipitates were eluted using acidic or basic elution buffers and analyzed by mass spectrometry (17). Polypeptide sequences from \sim 250 distinct proteins were identified using this methodology, including previously described binding partners such as vimentin, providing validation of the screen methodology (Table 1). We also found peptide sequences from histones (including histones H1.2, H2B, and H4), heat shock protein 70, ribosomal proteins (40S and 60S), and PARP1, as well as Prohibitin-2 and myristoylated alanine-rich protein kinase C substrate (MARCK), which have putative roles in invasion and metastasis (Fig. 1, Table 1) (8, 22–24). The most striking ATDC-interacting protein identified by this screen was RNF8 (37% peptide coverage by mass spectroscopy, Fig. 1), suggesting that ATDC and RNF8 are interaction partners. Of the putative interaction partners of ATDC, we decided to focus on RNF8 due to its known role in the DNA damage response and our prior data indicating a role for ATDC in IR resistance (25).

To confirm that the ATDC and RNF8 proteins physically associate, we next performed co-immunoprecipitation experiments using HEK 293 cells (which have low/absent endogenous ATDC expression), transfected with either empty vector or overexpressing FLAG-ATDC. RNF8 consistently co-immunoprecipitated with FLAG-ATDC (Fig. 2A). Immunoprecipitation of endogenous ATDC in BxPC3 pancreatic cancer cells that express high endogenous levels of ATDC also confirmed co-IP of endogenous RNF8 (Fig. 2B). To determine whether ATDC binds directly to RNF8, we performed GST pulldown assays and found that GST-RNF8 pulled down both immunoprecipitated FLAG-ATDC and *in vitro* translated FLAG-ATDC, indicating that the interaction between the proteins is direct (Fig. 2C). These results establish a novel and direct physical interaction between ATDC and RNF8.

The ATDC-RNF8 Interaction Is Mediated by the C Terminus of ATDC and the RING Domain of RNF8—To define the domains critical for the interaction between ATDC and RNF8, we first created a series of truncation mutants of FLAG-tagged ATDC (Fig. 3A). Co-IP of FLAG-tagged full-length and truncated ATDC proteins with RNF8 revealed that the deletion of the C terminus (Δ C) abolished the interaction of ATDC with RNF8 and that expression of the ATDC C terminus alone (ATDC Δ 348) was sufficient to mediate interaction with RNF8 (Fig. 3, B and C). To identify whether the FHA or RING domains of RNF8 were required for interaction with ATDC, we created Myc-tagged constructs lacking these domains (Fig. 4A), which were then transfected and co-expressed with ATDC in HEK 293 cells (Fig. 4, B and C). Although deletion of the RNF8 FHA domain (Δ FHA) did not disrupt interaction with ATDC, loss of the RING domain (Δ RING) of RNF8 completely blocked the interaction with ATDC, demonstrating that the RING domain of RNF8 is required for ATDC binding (Fig. 4B). These

TABLE 1
Putative ATDC/TRIM29-interacting proteins identified by mass spectroscopy

Shown are the top 28 polypeptide sequences identified from ATDC immunoprecipitates. Spectral Count refers to the number of unique peptide spectra mapping to the indicated protein.

| Protein | Accession number | Molecular weight | Spectral counts #1 ^a | Spectral counts #2 ^b |
|--|------------------|------------------|---------------------------------|---------------------------------|
| | | <i>kDa</i> | | |
| ATDC/TRIM29 | NP_036233 | 66 | 223 | 95 |
| Histone H1.2 | NP_005310 | 21 | 78 | 43 |
| Histone H2B type 1-C/E/F/G/I | NP_003517 | 14 | 69 | 19 |
| Heat shock 70 kDa protein 1A/1B | NP_005336 | 70 | 37 | 18 |
| Histone H4 | NP_003531 | 11 | 26 | 19 |
| Y-box-binding protein 3 | NP_003642 | 40 | 28 | 14 |
| Histone H2A type 1 | NP_003505 | 14 | 31 | 10 |
| Prohibitin-2 | NP_001138303 | 33 | 22 | 15 |
| E3 ubiquitin-protein ligase RNF8 | NP_003949 | 56 | 0 | 36 |
| Vimentin | NP_003371 | 54 | 20 | 9 |
| 60S ribosomal protein L13 | NP_150254 | 24 | 21 | 8 |
| 40S ribosomal protein S19 | NP_001013 | 16 | 17 | 10 |
| Brain acid-soluble protein 1 | NP_001258535 | 23 | 3 | 22 |
| 78-kDa glucose-regulated protein precursor (GRP78) | NP_005338 | 72 | 25 | 5 |
| 40S ribosomal protein S4, X isoform X isoform | NP_000998 | 30 | 17 | 7 |
| 40S ribosomal protein S18 | NP_072045 | 18 | 14 | 8 |
| Histone H1x | NP_006017 | 22 | 14 | 8 |
| Plasminogen activator inhibitor 1 RNA-binding protein | NP_001018077 | 51 | 19 | 3 |
| 40S ribosomal protein S10 | NP_001191020 | 19 | 15 | 6 |
| Complement component 1 Q subcomponent-binding protein, mitochondrial precursor | NP_001203 | 31 | 18 | 3 |
| High mobility group protein HMG-1/HMG-Y | NP_665908 | 12 | 13 | 8 |
| Myristoylated alanine-rich C-kinase substrate | NP_002347 | 32 | 8 | 12 |
| Histone H1.0 | NP_032223 | 21 | 16 | 4 |
| Heterogeneous nuclear ribonucleoprotein U | NP_114032 | 89 | 8 | 11 |
| 60S ribosomal protein L26 | NP_000978 | 17 | 12 | 7 |
| Elongation factor 1- α | NP_001393 | 50 | 0 | 66 |
| PARP1 | NP_001609 | 113 | 6 | 8 |
| RuvB-like 2 | NP_006657 | 51 | 12 | 0 |

^a Protein elution using 50 mM ethanolamine buffer, pH 11.5.

^b Protein elution using 50 mM glycine buffer, pH 2.5.

results define a novel interaction between the C terminus of ATDC and the RING domain of RNF8.

We have previously characterized phosphorylation of ATDC on the Ser-550 residue as a critical determinant of the radioprotective function of ATDC, which is mediated by MAPKAPK2 (25). This residue maps to the C-terminal interaction domain of ATDC, and so we hypothesized that the interaction between ATDC and RNF8 might require this Ser-550 residue. To determine this, we performed co-IP experiments in HEK 293 lysates co-expressing RNF8 and either WT ATDC or ATDC S550A mutant proteins. We observed that mutation of Ser-550 to alanine abrogated ATDC co-IP with RNF8 (Fig. 4C). The RING domain of RNF8 is required for its ubiquitin ligase function as well as interaction with ATDC (Fig. 4B). The typical function of RING domains is ubiquitin ligation. Mutation of the RNF8 RING domain Cys-403 residue to Ser blocks ligation function. To determine whether the ubiquitin ligase function of RNF8 was required for the ATDC-RNF8 interaction, we also performed co-IP with RNF8 C403S mutant protein. RNF8 C403S co-immunoprecipitated with ATDC (Fig. 4C), indicating that ligation function was dispensable for the RNF8-ATDC interaction.

To further confirm that the RNF8-ATDC interaction occurs under physiologic conditions, we expressed RNF8 and its Δ FHA and Δ RING truncation mutant proteins in UC14 and CAPAN2 tumor cells, which have endogenous ATDC expression. As seen in HEK 293, wild type, but not Δ RING RNF8, co-immunoprecipitated with endogenous ATDC (Fig. 4D). Taken together, these data demonstrate that the C terminus of ATDC interacts with the RING domain of RNF8 and that this

interaction requires the Ser-550 residue of ATDC, but not the RNF8 ubiquitin ligase function.

ATDC Is Present in the Cytoplasm and Nucleus and Requires Its Coiled-coil Domain for Nuclear Shuttling—ATDC has previously been reported to localize predominantly to the cytoplasm and cytoskeleton of cells (10). Other groups have reported that in certain cell lines, it is predominately present in the nucleus (18). RNF8 has been shown to have nuclear localization and to localize to sites of DNA damage after irradiation (4). Because ATDC expression leads to resistance to multiple forms of DNA damage, including IR, and because we demonstrated a physical interaction between these molecules, we next wanted to determine where ATDC and RNF8 interact within cells (25). Under basal conditions, RNF8 localized exclusively to the nuclear fraction when overexpressed in HEK 293 cells (Fig. 5A), whereas ATDC was present in cytoplasmic, cytoskeletal, and nuclear fractions in both HEK 293 cells (Fig. 5B) and the pancreatic cell line BxPC3 (Fig. 5C), which has high endogenous levels of ATDC. To confirm that ATDC localized to the cytoplasm and the nucleus, cells expressing ATDC were immunostained and examined by confocal microscopy. Although ATDC was predominately cytoplasmic, 20% was nuclear, confirming the cell fractionation experiments (Fig. 5D). To explore whether certain domains of ATDC were responsible for nuclear localization of ATDC, HEK 293 cells stably transfected with full-length or truncated FLAG-ATDC mutants were examined by cell protein fractionation. Interestingly, although loss of the ATDC C terminus, which binds to RNF8 (ATDC Δ C), did not block trafficking to the nucleus, loss of the coiled-coil domain (ATDC Δ 348) did block detection of ATDC in the nucleus (Fig.

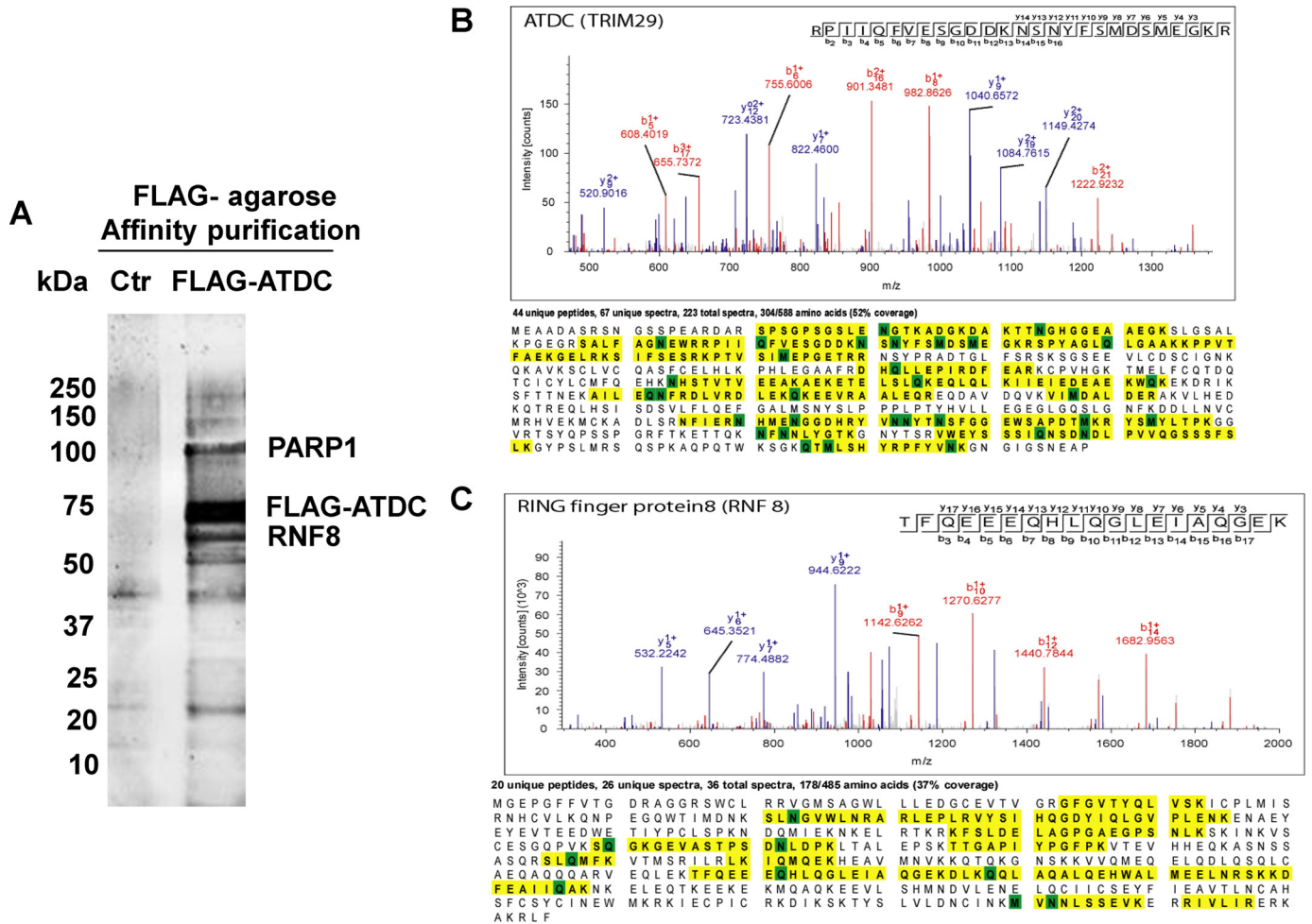


FIGURE 1. Analysis of ATDC protein binding partners using affinity purification and mass spectroscopy. A, Coomassie Blue-stained gel demonstrating total proteins affinity-purified with ATDC in HEK 293 cells transfected with empty vector (Ctr) or FLAG-ATDC expression vector. PARP1 and RNF8 bands are indicated. B and C, each protein, ATDC (B) and RNF8 (C), was identified with sequence coverage using MS analysis.

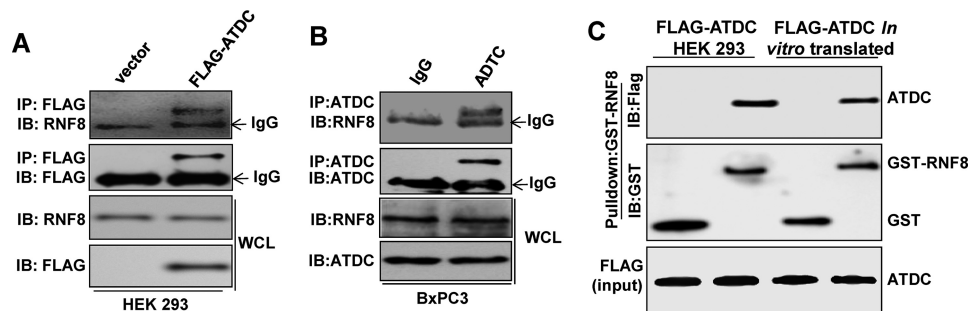


FIGURE 2. ATDC interacts directly with RNF8. A, co-immunoprecipitation of endogenous RNF8 with FLAG-tagged ATDC in HEK 293 cells. B, immunoblot. WCL, whole cell lysate. C, GST pull-down assays identify direct protein interaction between GST-RNF8 and FLAG-ATDC or *in vitro* translated FLAG-ATDC protein.

5E). These results reveal that ~20% of ATDC is present in the nucleus and that trafficking of ATDC to the nucleus requires its coiled-coil domain but not the C-terminal RNF8 interaction domain.

Ionizing Radiation Increases ATDC Nuclear Trafficking and Binding to RNF8—We next hypothesized that IR may induce ATDC translocation to the nucleus and promote binding to RNF8, facilitating DNA repair. To determine whether IR induces ATDC nuclear translocation, HEK 293 cells expressing ATDC or ATDCΔC were treated with IR (10 Gy) and the cytoplasmic and

nuclear fractions were isolated at various time points (1, 3, 6, and 24 h) following IR. We observed an increase in ATDC in the nuclear fraction starting at 1 h and increasing until 24 h after IR, which also corresponded to a decrease in the cytoplasmic portion of ATDC (Fig. 6A, top three panels). Similar results were seen with the ATDCΔC construct, indicating that IR induces ATDC trafficking to the nucleus and that this process does not require the C terminus of ATDC (Fig. 6A, bottom three panels).

To determine whether IR also promoted the ATDC-RNF8 interaction, we next performed co-immunoprecipitation of

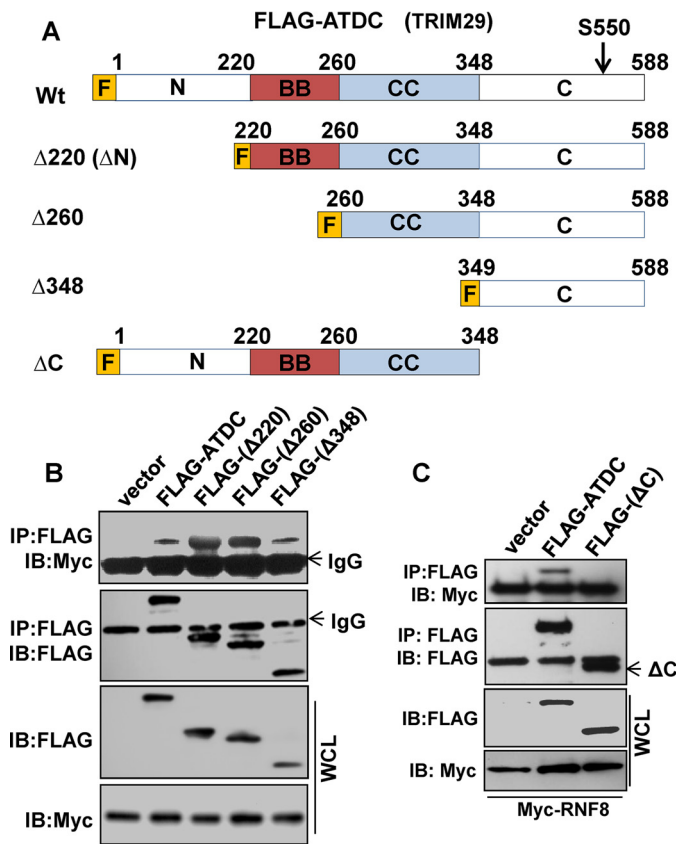


FIGURE 3. Identification of RNF8 interaction domains of ATDC. *A*, FLAG-ATDC truncation/deletion constructs. *B*, co-IP between RNF8 and ATDC truncation mutants identifies the C terminus of ATDC (ATDC Δ 348) as the minimal domain of ATDC required for interaction with RNF8. *B*, immunoblot; WCL, whole cell lysate. *C*, deletion of C-terminal amino acids 349–588 blocked co-IP with RNF8.

Myc-RNF8 and FLAG-ATDC in cells before and 1 or 3 h after irradiation with 10 Gy. Treatment with IR increased ATDC pulldown with RNF8 at 1 h after irradiation, but this increase returned to baseline levels by 3 h (Fig. 6B). Conversely, immunoprecipitation of FLAG-ATDC or FLAG-ATDC Δ C from whole cell extracts following irradiation resulted in increased pulldown of RNF8 by wild type ATDC, but not ATDC Δ C, confirming the importance of the ATDC C terminus for RNF8 binding (Fig. 6C).

RNF8 is recruited to nuclear DNA repair foci (marked by H2AX phosphorylation) following IR (1). Given that ATDC is recruited to the nucleus and binds to RNF8, we hypothesized that ATDC might be recruited to IR-induced foci. To examine this, we immunostained BxPC3 cells before and after IR for expression of γ -H2AX and ATDC. Although we observed formation of numerous γ -H2AX foci, we did not observe ATDC recruitment to the IR-induced H2AX foci (Fig. 7A). To further confirm the lack of ATDC recruitment to DNA damage foci, we transfected Panc1 cells with GFP-ATDC and microlaser-irradiated cells, a mechanism to induce high levels of localized DNA damage. Although GFP-RNF8 is rapidly recruited to laser-irradiated DNA damage tracts, we found no evidence that ATDC accumulated at sites of DNA damage (Fig. 7, B and C) (1).

Although ATDC is not recruited to sites of DNA damage, we postulated that it may influence the kinetics of RNF8 recruit-

ment to the chromatin, and thus influence the DNA damage response. To test this, we examined recruitment of RNF8 and ATDC to chromatin following IR. In control cells lacking ATDC, RNF8 was rapidly (by 1 h) and persistently (>24 h) recruited to the chromatin (Fig. 6D, top panels). In contrast, in ATDC-expressing HEK 293 cells, RNF8 chromatin loading was less rapid (peak at 6 h) and returned to basal levels by 24 h (Fig. 6D, middle panels). Furthermore, although ATDC was not recruited to DNA damage sites, IR did induce ATDC loading to chromatin with similar kinetics to RNF8 (Fig. 6D). Deletion of the ATDC RNF8 binding domain reduced association of ATDC with chromatin, suggesting that ATDC loading to chromatin is dependent on interaction with RNF8 (Fig. 6D, bottom panels). Taken together, these results establish ATDC nuclear trafficking and binding to RNF8 as a regulator of ATDC recruitment and binding to chromatin following exposure to IR and suggest that this interaction may influence the stability of RNF8 binding to chromatin following DNA damage.

ATDC-mediated Radioresistance Requires Both N Terminal and C Terminal Regions—We have previously shown that ATDC expression leads to enhanced growth and resistance to IR and that knockdown or loss of ATDC sensitizes cells to IR (17, 25). Others have demonstrated that knockdown of ATDC sensitizes cells to UV irradiation (26). ATDC has also been reported to interact with p53 through its N terminus and to inhibit p53 nuclear activity (10). To confirm the importance of ATDC for radioresistance, we next investigated the survival rate of HEK 293 cells with stable expression of full-length ATDC, ATDC Δ 220(Δ N), or ATDC Δ C (Fig. 8A). Interestingly, although full-length ATDC increased resistance to IR as expected, cells expressing either of the ATDC truncation mutants ATDC Δ N or ATDC Δ C showed a partial resistance to IR (*versus* full-length ATDC) but still had a significant increase in survival when compared with HEK 293 cells lacking ATDC (Fig. 8, B and C). These data indicate that both the N termini and the C termini of ATDC participate in protection against IR.

The primary cytotoxic lesion induced by IR is DNA DSBs. To examine whether the radioprotective effect of ATDC correlated with increased DNA DSB repair, we used neutral comet assays to measure whether ATDC expression altered accumulation and resolution of DSBs. When compared with control cells, cells stably expressing ATDC showed shorter comet tails 6 h after exposure to IR, and this effect was more pronounced 24 h after IR (Fig. 8D), suggesting that expression of ATDC increased the kinetics of DNA repair. In contrast, cells expressing ATDC Δ C (which lack the ability to bind RNF8) showed no significant change in length of comet tails when compared with control cells (Fig. 8, D and E). These results indicate that ATDC promotes radioresistance by improved DNA DSB repair kinetics and that this effect requires its C-terminal RNF8 interaction domain.

ATDC Promotes IR-induced γ -H2AX Ubiquitination, 53BP1 Phosphorylation, and Resolution of DNA Damage Foci following DNA Damage—RNF8 promotes repair by mono-ubiquitination of γ -H2AX and recruitment of DNA repair proteins such as 53BP1 and BRCA1 to IR-induced DNA DSB sites (3, 4). To investigate whether the interaction between ATDC and RNF8 modulated RNF8 function following DNA damage, we exam-

ATDC Interaction with RNF8

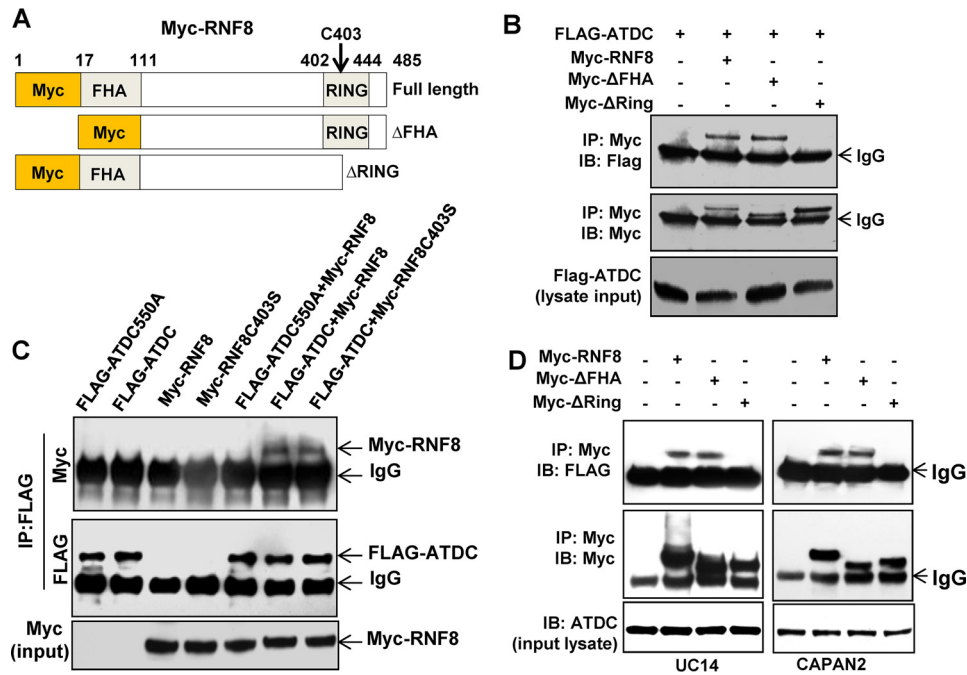


FIGURE 4. Identification of ATDC interaction domains of RNF8. *A*, Myc-RNF8 truncation and deletion constructs. *B*, the RING domain of RNF8 is required for co-IP with ATDC. *IB*, immunoblot. *C*, mutation of the RNF8 catalytic Cys-403 residue to Ser does not block co-IP with ATDC. *D*, wild type (Myc-RNF8) and Δ FHA (Myc- Δ FHA), but not Δ RING (Myc- Δ RING) RNF8 supported co-IP with endogenous ATDC in two separate tumor cell lines (UC14, bladder cancer, and CAPAN2, pancreatic cancer).

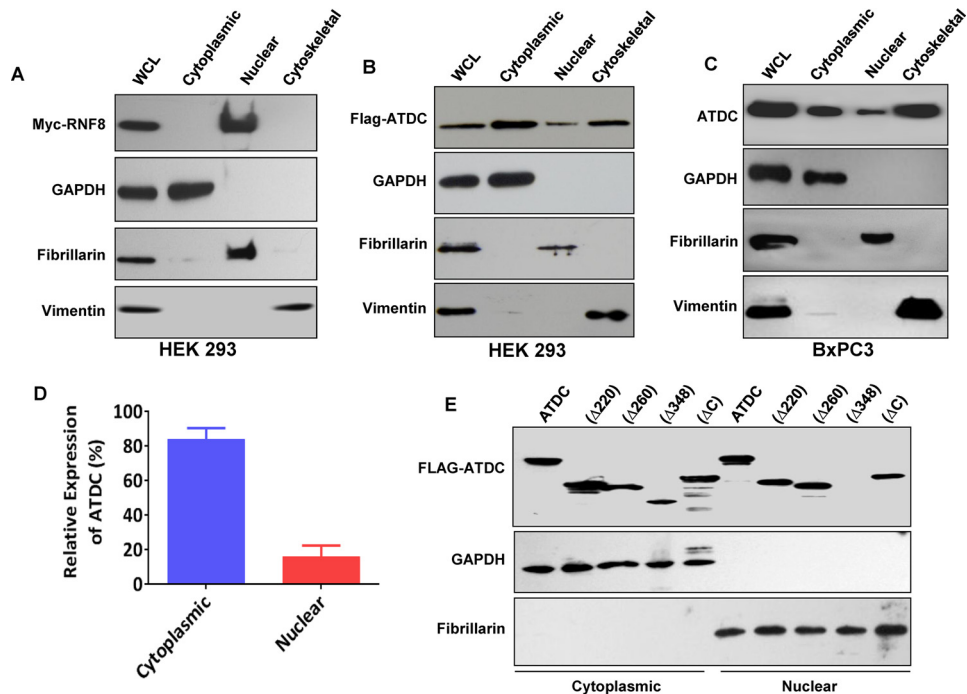


FIGURE 5. ATDC is detectable in both the cytoplasm and the nucleus. *A*, HEK 293 cells with stable expression of Myc-RNF8 demonstrate nuclear localization of RNF8. *WCL*, whole cell lysate. *B*, HEK 293 with stable expression of FLAG-ATDC demonstrates cytoplasmic, nuclear, and cytoskeletal localization of ATDC. *C*, endogenous ATDC in BxPC3 cells also localizes to the cytoplasmic, nuclear, and cytoskeletal fractions. *D*, cellular localization of FLAG-ATDC by confocal microscopy demonstrated that 80% of ATDC is localized in the cytoplasm and 20% is localized in the nucleus. *Error bars* = mean \pm S.D. *E*, ATDC Δ 348, which lacks the coiled-coil region of ATDC, does not localize to the nucleus.

ined whether ATDC expression altered IR-induced, RNF8-mediated γ -H2AX ubiquitination. Interestingly, ATDC (but not ATDC Δ C) expression up-regulated RNF8-mediated IR-induced γ -H2AX mono-ubiquitination at 30 and 60 min after IR (Fig. 9, *A* and *B*).

The ubiquitin ligase function of RNF8 promotes phosphorylation of 53BP1 and its recruitment to DNA DSB repair foci (27). To determine whether the RNF8-ATDC interaction promoted phosphorylation of 53BP1 following IR, we measured phospho-53BP1 levels following IR in cells with ATDC,

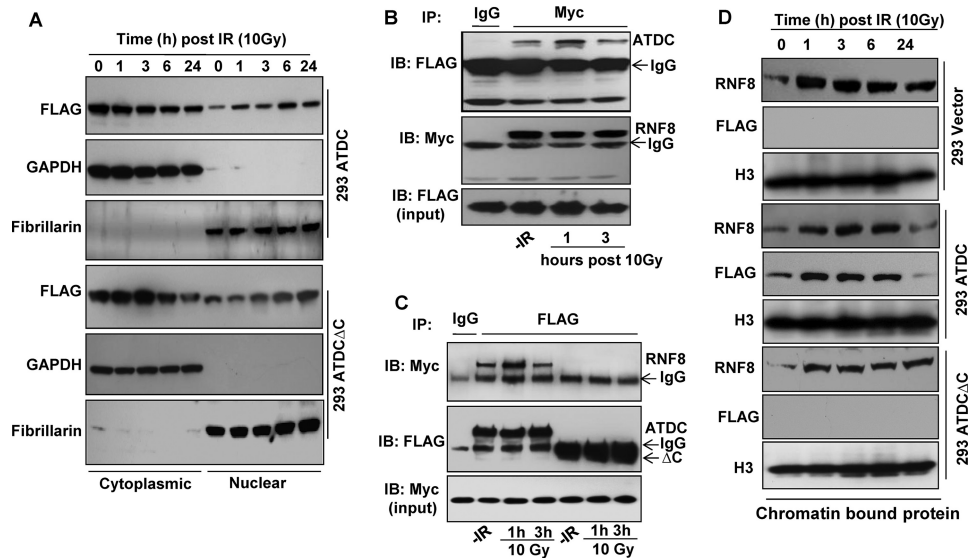


FIGURE 6. Ionizing radiation promotes ATDC translocation to the nucleus and binding to RNF8. *A*, IR induced increasing levels of ATDC in the nuclear fraction and was not affected by C-terminal deletion of ATDC. *B*, IR induced increased co-IP of FLAG-ATDC and RNF8 1 h after irradiation. *B*, immunoblot. *C*, IR induced increased co-IP of Myc-RNF8 and ATDC (but not ATDC Δ C) 1 h after irradiation. *D*, ATDC expression reduces the chromatin-bound fraction of RNF8 following IR.

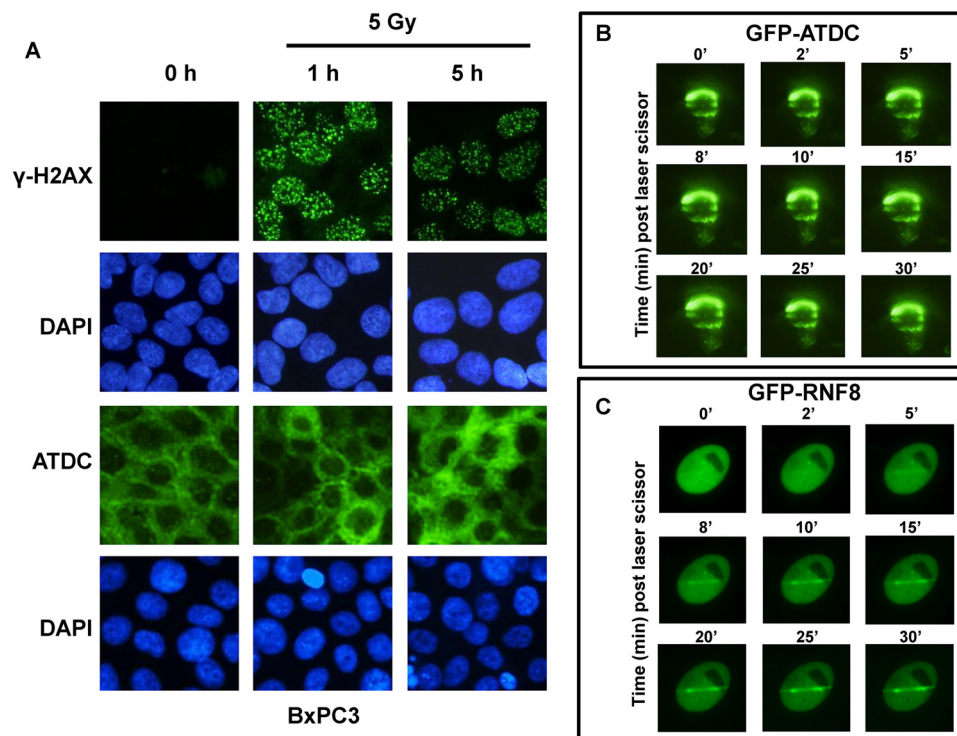


FIGURE 7. ATDC does not localize to DNA repair foci. *A*, immunofluorescent staining of BxPC3 cells demonstrated numerous H2AX foci 1 and 5 h after IR, but no co-localization of ATDC. *B*, GFP-tagged ATDC (GFP-ATDC) does not co-localize to laser-irradiated DNA damage tracts. *C*, GFP-RNF8 rapidly localizes to laser-irradiated DNA damage tracts.

ATDC Δ C, or no ATDC (Fig. 9, *C* and *D*). Expression of full-length ATDC, but not ATDC Δ C, promoted increased phosphorylation of 53BP1 following IR. These data suggest that the interaction of ATDC with RNF8 influences RNF8-mediated γ -H2AX mono-ubiquitination and enhances phosphorylation of 53BP1 in response to IR.

Phosphorylation of H2AX occurs rapidly following induction of DNA DSB and is a marker of persistent DNA damage (28). To assess the effect of the ATDC-RNF8 interaction on

IR-induced H2AX phosphorylation, HEK 293 cells with and without ATDC or ATDC Δ C were treated with IR (10 Gy) and H2AX phosphorylation and mono-ubiquitination was measured by Western blotting. As seen in Fig. 9A, ATDC expression promoted mono-ubiquitination following IR (Fig. 10A). In control vector- and ATDC Δ C-expressing cells, IR treatment also resulted in H2AX phosphorylation (γ H2AX band) after as early as 10 min, which persisted for 24 h (Fig. 10). Irradiation of ATDC-expressing cells resulted in a similar pattern of induc-

ATDC Interaction with RNF8

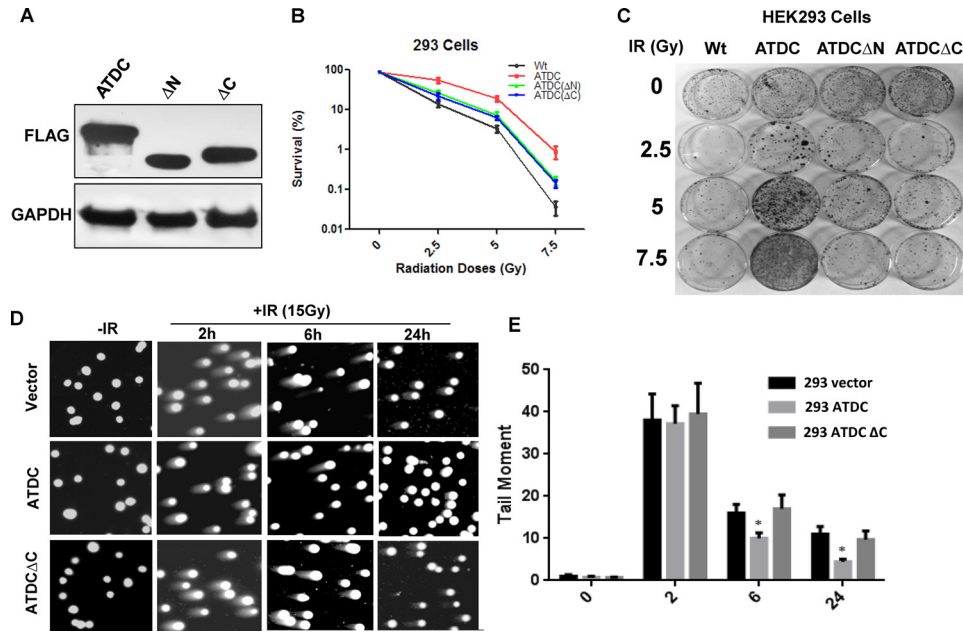


FIGURE 8. ATDC protects cells against IR. *A*, Western blotting demonstrates stable and comparable expression of wild type, ATDCΔN, and ATDCΔC constructs in HEK 293 cells. *B* and *C*, clonogenic cell survival assays following IR in HEK 293 cells stably expressing wild type ATDC, ATDCΔN, or ATDCΔC demonstrate that only wild type ATDC fully protects cells from IR. The results are shown from three independent experiments (mean ± S.D., *, $p < 0.05$ versus control). *D* and *E*, ATDC wild type but not ATDCΔC promoted repair of DNA DSBs as measured by neutral comet assays as shown by representative images (*D*) and quantitation of tail moments (mean ± S.D., *, $p < 0.05$ versus vector control) (*E*).

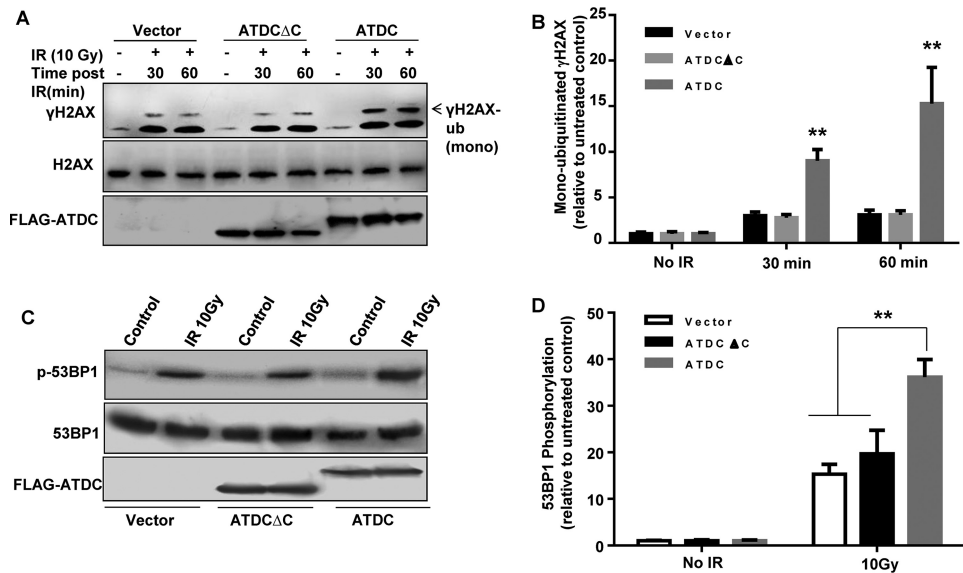


FIGURE 9. ATDC promotes IR induced γ H2AX mono-ubiquitination and 53BP1 phosphorylation following IR. *A*, wild type ATDC, but not ATDCΔC, promoted mono-ubiquitination of γ H2AX (γ H2AX-ub (mono)) following IR (10 Gy) as measured by Western blot. *B*, quantitation of -fold increase in mono-ubiquitination of γ H2AX normalized to H2AX relative to untreated control (mean ± S.D., **, $p < 0.05$ versus vector control). *C*, wild type ATDC, but not ATDCΔC, enhanced 53BP1 phosphorylation (p -53BP1) as measured by Western blot. *D*, quantitation of -fold increase in phosphorylation of 53BP1 normalized to unphosphorylated 53BP1 and relative to untreated control (mean ± S.D., **, $p < 0.05$ versus vector control).

tion of H2AX phosphorylation, but a more rapid return to basal levels after 3 h (Fig. 10, *B* and *C*).

H2AX and BRCA1 DNA damage foci are markers of DNA DSBs. To examine whether ATDC and ATDCΔC influenced kinetics of foci formation and resolution, we stained HEK 293 cells without and with either ATDC or ATDCΔC following IR (Fig. 11). We noted that RNF8 and BRCA1 formed nuclear foci rapidly with similar numbers of foci and fluorescence intensity in both ATDC-expressing and control cells 1 h following IR (4 Gy) (Fig. 11, data not shown). However,

ATDC-expressing cells had a more rapid resolution of the RNF8 and BRCA1 foci at the 6-h time point after IR and almost complete resolution of foci at 24 h. In contrast, ATDCΔC stably expressing cells showed no difference in the time course of foci recovery when compared with control cells lacking ATDC (Fig. 11, *B* and *C*). These results show that the interaction between ATDC and RNF8 enhances recovery of DNA damage and correlates with enhanced resolution of H2AX phosphorylation and RNF8/BRCA1 foci following IR in a time-dependent manner.

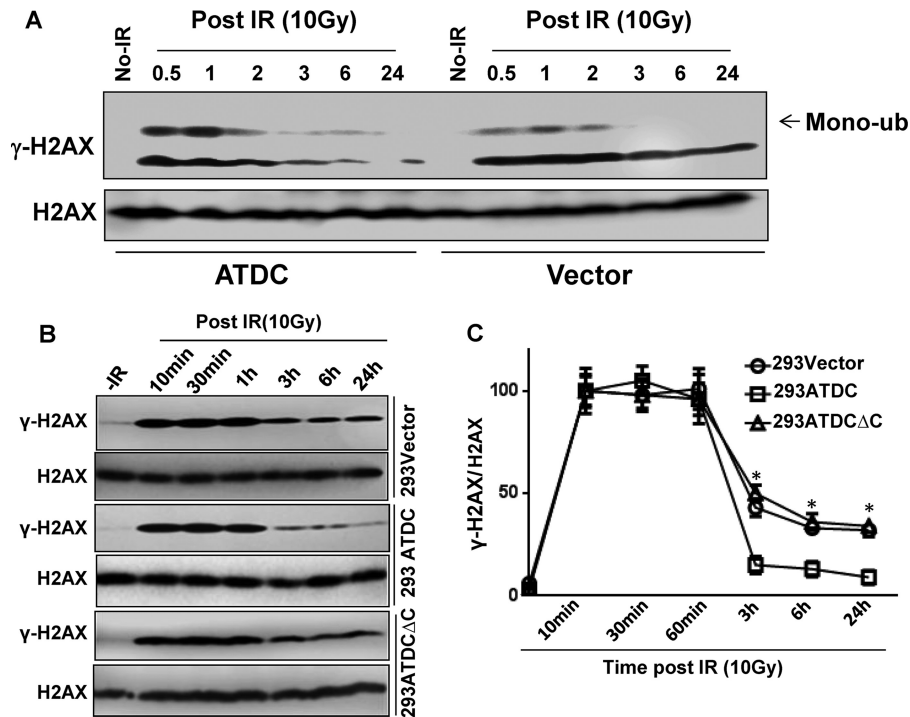


FIGURE 10. **ATDC promotes dephosphorylation of H2AX following IR.** *A*, ATDC expression promoted both increased ubiquitination of γ H2AX and more rapid dephosphorylation of H2AX following IR as measured by Western blot. *Mono-ub*, mono-ubiquitination. *B*, ATDC Δ C does not promote dephosphorylation of H2AX (mono-ubiquitination band not shown). *C*, quantitation of *B* ($n = 3$, mean \pm S.D., *, $p < 0.05$ versus vector control).

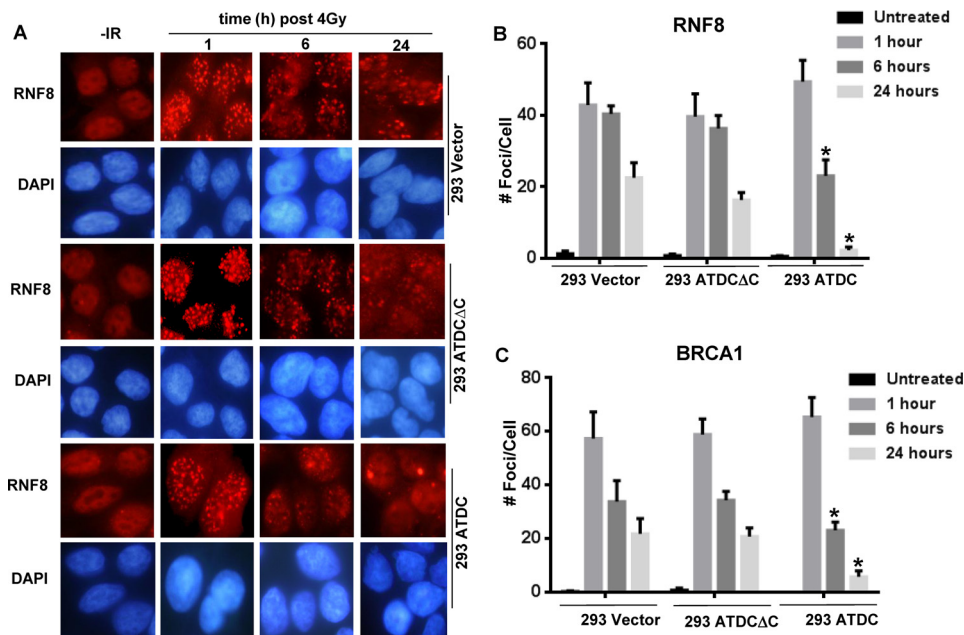


FIGURE 11. **Expression of ATDC promoted RNF8 and BRCA1 DNA repair foci resolution.** *A*, immunofluorescent staining for RNF8 following treatment with 4 Gy IR. *B* and *C*, cells expressing ATDC or ATDC Δ C were treated with IR for various time points, and RNF8 (*B*) and BRCA1 (*C*) foci were quantitated. *Error bars* = S.E. *, $p < 0.01$ when compared with vector or ATDC Δ C controls.

Discussion

DNA damage-induced cell death is an integral component of anticancer therapy. Understanding the DNA damage response that restores genomic integrity following cancer cell treatment and thus mitigates cell death is essential to understand therapy resistance and develop ways to reverse it. We have previously reported that ATDC becomes phosphorylated by MK2 downstream of p38 and ATM and induces resistance to IR, but the

downstream mechanism(s) by which ATDC provides resistance to IR-induced DNA damage remained elusive (25). To identify potential downstream effectors, we performed a mass spectrometry-based screen for proteins that physically interact with ATDC. This screen identified the DNA repair factor, RNF8, as a putative binding partner for ATDC (3, 4). In this study, we confirm that ATDC shares a direct physical contact with RNF8 that is enhanced following induction of DNA dam-

ATDC Interaction with RNF8

age. We have further refined the interaction domains of these proteins to the C terminus of ATDC and the RING domain of RNF8 and demonstrate that the interaction requires the ATDC Ser-550 residue (which is phosphorylated following IR) but is not dependent on the ubiquitin ligase function of RNF8. Furthermore, we demonstrate that this interaction results in improved DNA DSB repair kinetics as measured by neutral comet assays, increased clonogenic survival, and a more rapid resolution of DNA repair foci following exposure to IR. These results establish the ATDC-RNF8 interaction as a key mechanism of ATDC-induced resistance to IR.

ATDC has previously been described as a driver of resistance to DNA damage by UV and ionizing radiation that binds to chromatin, but the exact means by which it promotes resistance to DNA damage was unclear (18, 25, 26). Like ATDC, RNF8 is activated in an ATM-dependent manner and participates in DDR by facilitating DNA DSB processing through ubiquitination of histones and DNA repair factors promoting the assembly of DNA repair complexes at sites of DNA DSB (3, 4). Here we characterize a direct interaction between ATDC and RNF8 that is enhanced by exposure to IR and that contributes to ATDC-induced IR resistance. Interestingly, the RNF8-ATDC interaction depended on the ATDC Ser-550 residue, which we have previously shown to be phosphorylated by MK2 downstream of ATM and which is required for the role of ATDC in radioresistance (25). We also find that although ATDC is predominantly cytoplasmic in most cell lines expressing it, some ATDC is present in the nucleus. Unexpectedly, ATDC does not itself appear to localize to nuclear repair foci but does bind to the chromatin and influence RNF8 chromatin binding following induction of DNA damage (Fig. 6D). These findings suggest that the ATDC-RNF8 interaction may have a more global effect on RNF8 nuclear dynamics, which occurs outside of the DNA repair foci but which is nonetheless important for efficient DNA repair (Table 1). These results are also consistent with a recent study identifying ATDC/TRIM29 as a nuclear DDR participant that binds to the chromatin following DNA damage (18).

RNF8 and its partner RNF168 are RING domain-containing ubiquitin ligases that are recruited to DNA DSB following H2AX phosphorylation by MDC1 (29). Following DNA damage, RNF8 and RNF168 catalyze the addition of ubiquitin to H2A and H2AX and recruitment of 53BP1 and BRCA1 to DNA damage sites, facilitating repair. Although the ATDC-RNF8 interaction does not influence initial RNF8 or BRCA1 foci formation, it did result in faster disappearance of these foci, suggesting that it speeds DNA DSB repair processes. Although the exact means by which the ATDC-RNF8 interaction impacts the function of RNF8 is incompletely understood, ATDC is known to bind the acetyltransferase Tip60, which is involved in chromatin remodeling and promotes RNF8 ubiquitin ligase activity and DNA repair (12, 30). Furthermore, our mass spectrometry screen also identified a putative interaction between ATDC and RuvBL2 (Tip48), another member of the p400/NuA4 complex that modulates RNF8 activity (Table 1) (18). We therefore hypothesize that ATDC may promote RNF8 activity, perhaps by physically binding to and coordinating the activity of the

chromatin-remodeling complexes necessary for RNF8 to promote efficient DNA DSB repair.

Although ATDC is important for cell survival, proliferation, and DNA DSB repair, it is notable that it lacks intrinsic enzymatic function. Indeed, ATDC seems to function as a direct protein link between proteins involved in DNA damage sensing (ATM-p38-MK2) and cell cycle regulation (DVL2, p53) (10, 17, 25). These results implicate RNF8 as an additional binding partner that influences DNA repair and resistance to damage. Together these findings suggest ATDC as a multifunctional scaffold protein that undergoes covalent modifications (phosphorylation, acetylation) following cellular insults and subsequently binds to multiple proteins in the cytoplasm and nucleus to coordinate cellular survival and DNA repair (10, 17, 25).

Induction of DNA damage leading to apoptosis and cell death by agents such as chemotherapy and ionizing radiation remains a critical aspect of modern cancer treatments. ATDC is highly expressed in many tumor types, binds to the DNA repair factor RNF8 and thus may be a determinant of resistance to both cytotoxic chemotherapy and ionizing radiation. RNF8 is required for robust DNA DSB repair, is expressed in many tumors, and appears to participate in acquired resistance to PARP inhibition (COSMIC (Catalogue of Somatic Mutations in Cancer)) (31). The identification of this novel interaction between ATDC and RNF8 establishes a new mechanism whereby ATDC and RNF8 could function in a coordinate manner to produce resistance to DNA damage-based anticancer therapies. Expression of these proteins may represent prognostic biomarkers that, if targeted, could result in tumor sensitization to therapy.

Author Contributions—H. Y., P. L. P., and D. M. S. designed, conducted, and analyzed the experiments and wrote the paper. L. W., G. M. N., C. L., and E. H. K. participated in individual experiments. J. P., D. E. M., X. Y., and M. L. participated in experimental design and interpretation of data.

References

1. Pinder, J. B., Attwood, K. M., and Dellaire, G. (2013) Reading, writing, and repair: the role of ubiquitin and the ubiquitin-like proteins in DNA damage signaling and repair. *Front. Genet.* **4**, 45
2. Jackson, S. P., and Durocher, D. (2013) Regulation of DNA damage responses by ubiquitin and SUMO. *Mol. Cell* **49**, 795–807
3. Mailand, N., Bekker-Jensen, S., Faustrup, H., Melander, F., Bartek, J., Lukas, C., and Lukas, J. (2007) RNF8 ubiquitylates histones at DNA double-strand breaks and promotes assembly of repair proteins. *Cell* **131**, 887–900
4. Huen, M. S., Grant, R., Manke, I., Minn, K., Yu, X., Yaffe, M. B., and Chen, J. (2007) RNF8 transduces the DNA-damage signal via histone ubiquitylation and checkpoint protein assembly. *Cell* **131**, 901–914
5. Wang, B., and Elledge, S. J. (2007) Ubc13/Rnf8 ubiquitin ligases control foci formation of the Rap80/Abxaxas/Brca1/Brc36 complex in response to DNA damage. *Proc. Natl. Acad. Sci. U.S.A.* **104**, 20759–20763
6. Leonhardt, E. A., Kapp, L. N., Young, B. R., and Murnane, J. P. (1994) Nucleotide sequence analysis of a candidate gene for ataxia-telangiectasia group D (ATDC). *Genomics* **19**, 130–136
7. Meroni, G. (2012) Genomics and evolution of the TRIM gene family. *Adv. Exp. Med. Biol.* **770**, 1–9
8. Brzoska, P. M., Chen, H., Zhu, Y., Levin, N. A., Disatnik, M. H., Mochly-Rosen, D., Murnane, J. P., and Christman, M. F. (1995) The product of the ataxia-telangiectasia group D complementing gene, ATDC, interacts with

- a protein kinase C substrate and inhibitor. *Proc. Natl. Acad. Sci. U.S.A.* **92**, 7824–7828
9. Yuan, Z., Peng, L., Radhakrishnan, R., and Seto, E. (2010) Histone deacetylase 9 (HDAC9) regulates the functions of the ATDC (TRIM29) protein. *J. Biol. Chem.* **285**, 39329–39338
 10. Yuan, Z., Villagra, A., Peng, L., Coppola, D., Glozak, M., Sotomayor, E. M., Chen, J., Lane, W. S., and Seto, E. (2010) The ATDC (TRIM29) protein binds p53 and antagonizes p53-mediated functions. *Mol. Cell. Biol.* **30**, 3004–3015
 11. Laderoute, K. R., Knapp, A. M., Green, C. J., Sutherland, R. M., and Kapp, L. N. (1996) Expression of the ATDC (ataxia telangiectasia group D-complementing) gene in A431 human squamous carcinoma cells. *Int. J. Cancer* **66**, 772–778
 12. Sho, T., Tsukiyama, T., Sato, T., Kondo, T., Cheng, J., Saku, T., Asaka, M., and Hatakeyama, S. (2011) TRIM29 negatively regulates p53 via inhibition of Tip60. *Biochim. Biophys. Acta* **1813**, 1245–1253
 13. Jiang, T., Tang, H. M., Lu, S., Yan, D. W., Yang, Y. X., and Peng, Z. H. (2013) Up-regulation of tripartite motif-containing 29 promotes cancer cell proliferation and predicts poor survival in colorectal cancer. *Med. Oncol.* **30**, 715
 14. Tang, Z. P., Dong, Q. Z., Cui, Q. Z., Papavassiliou, P., Wang, E. D., and Wang, E. H. (2013) Ataxia-telangiectasia group D complementing gene (ATDC) promotes lung cancer cell proliferation by activating NF- κ B pathway. *PLoS ONE* **8**, e63676
 15. Lai, W., Zhao, J., Zhang, C., Cui, D., Lin, J., He, Y., Zheng, H., Wu, X., and Yang, M. (2013) Upregulated ataxia-telangiectasia group D complementing gene correlates with poor prognosis in patients with esophageal squamous cell carcinoma. *Dis. Esophagus* **26**, 817–822
 16. Kosaka, Y., Inoue, H., Ohmachi, T., Yokoe, T., Matsumoto, T., Mimori, K., Tanaka, F., Watanabe, M., and Mori, M. (2007) Tripartite motif-containing 29 (TRIM29) is a novel marker for lymph node metastasis in gastric cancer. *Ann. Surg. Oncol.* **14**, 2543–2549
 17. Wang, L., Heidt, D. G., Lee, C. J., Yang, H., Logsdon, C. D., Zhang, L., Fearon, E. R., Ljungman, M., and Simeone, D. M. (2009) Oncogenic function of ATDC in pancreatic cancer through Wnt pathway activation and β -catenin stabilization. *Cancer Cell* **15**, 207–219
 18. Masuda, Y., Takahashi, H., Sato, S., Tomomori-Sato, C., Saraf, A., Washburn, M. P., Florens, L., Conaway, R. C., Conaway, J. W., and Hatakeyama, S. (2015) TRIM29 regulates the assembly of DNA repair proteins into damaged chromatin. *Nat. Commun.* **6**, 7299
 19. Chiong, E., Dadbin, A., Harris, L. D., Sabichi, A. L., and Grossman, H. B. (2009) The use of short tandem repeat profiling to characterize human bladder cancer cell lines. *J. Urol.* **181**, 2737–2748
 20. Lu, L. Y., Wu, J., Ye, L., Gavrilina, G. B., Saunders, T. L., and Yu, X. (2010) RNF8-dependent histone modifications regulate nucleosome removal during spermatogenesis. *Dev. Cell* **18**, 371–384
 21. Yang, H., and Mattingly, R. R. (2006) The Ras-GRF1 exchange factor coordinates activation of H-Ras and Rac1 to control neuronal morphology. *Mol. Biol. Cell* **17**, 2177–2189
 22. Chen, C. H., Chiu, C. L., Adler, K. B., and Wu, R. (2014) A novel predictor of cancer malignancy: up-regulation of myristoylated alanine-rich C kinase substrate phosphorylation in lung cancer. *Am. J. Respir. Crit. Care Med.* **189**, 1002–1004
 23. Hanada, S., Takehashi, A., Nishiyama, N., Wei, M., Yamano, S., Chung, K., Komatsu, H., Inoue, H., Suehiro, S., and Wanibuchi, H. (2013) Myristoylated alanine-rich C-kinase substrate as a prognostic biomarker in human primary lung squamous cell carcinoma. *Cancer Biomark.* **13**, 289–298
 24. Fu, P., Yang, Z., and Bach, L. A. (2013) Prohibitin-2 binding modulates insulin-like growth factor-binding protein-6 (IGFBP-6)-induced rhabdomyosarcoma cell migration. *J. Biol. Chem.* **288**, 29890–29900
 25. Wang, L., Yang, H., Palmbos, P. L., Ney, G., Detzler, T. A., Coleman, D., Leflein, J., Davis, M., Zhang, M., Tang, W., Hicks, J. K., Helchowski, C. M., Prasad, J., Lawrence, T. S., Xu, L., Yu, X., Canman, C. E., Ljungman, M., and Simeone, D. M. (2014) ATDC/TRIM29 phosphorylation by ATM/MAPKAP kinase 2 mediates radioresistance in pancreatic cancer cells. *Cancer Res.* **74**, 1778–1788
 26. Bertrand-Vallery, V., Belot, N., Dieu, M., Delaive, E., Ninane, N., Demazy, C., Raes, M., Salmon, M., Poumay, Y., Debacq-Chainiaux, F., and Toussein, O. (2010) Proteomic profiling of human keratinocytes undergoing UVB-induced alternative differentiation reveals TRIPartite Motif Protein 29 as a survival factor. *PLoS ONE* **5**, e10462
 27. Panier, S., and Durocher, D. (2009) Regulatory ubiquitylation in response to DNA double-strand breaks. *DNA Repair (Amst.)* **8**, 436–443
 28. Scully, R., and Xie, A. (2013) Double strand break repair functions of histone H2AX. *Mutat. Res.* **750**, 5–14
 29. Bartocci, C., and Denchi, E. L. (2013) Put a RING on it: regulation and inhibition of RNF8 and RNF168 RING finger E3 ligases at DNA damage sites. *Front. Genet.* **4**, 128
 30. Xu, Y., Sun, Y., Jiang, X., Ayrappetov, M. K., Moskwa, P., Yang, S., Weinstein, D. M., and Price, B. D. (2010) The p400 ATPase regulates nucleosome stability and chromatin ubiquitination during DNA repair. *J. Cell Biol.* **191**, 31–43
 31. Xu, G., Chapman, J. R., Brandsma, I., Yuan, J., Mistrik, M., Bouwman, P., Bartkova, J., Gogola, E., Warmerdam, D., Barazas, M., Jaspers, J. E., Watanabe, K., Pieterse, M., Kersbergen, A., Sol, W., Celie, P. H., Schouten, P. C., van den Broek, B., Salman, A., Nieuwland, M., de Rink, I., de Ronde, J., Jalink, K., Boulton, S. J., Chen, J., van Gent, D. C., Bartek, J., Jonkers, J., Borst, P., and Rottenberg, S. (2015) REV7 counteracts DNA double-strand break resection and affects PARP inhibition. *Nature* **521**, 541–544